Journal of the Association of Arab Universities for Basic and Applied Sciences (2015) 18, 12–18

University of Bahrain

Journal of the Association of Arab Universities for Basic and Applied Sciences

www.elsevier.com/locate/jaaubas
www.sciencedirect.com

تأثير لدينة ثلاثية المكونات(الأنيلين– فورمالدهيد والبيبيرازين) على تآكل الفولاذ الطري في وسط حمض الهيدروكلوريك

K. R. Ansari, M. A. Quraishi*

Department of Chemistry, Indian Institute of Technology, Banaras Hindu University, Varanasi 221005, India.

الملخص:

تم تحضير لدينة من نوع قاعدة شيف تحتوي على الأنيلين– فورمالدهيد والبيبرازين (AFPP) ودراسة استخدامها كمانع لتآكل الفولاذ الطري في وسط حمض الكلوريك المولاري عن طريق قياس فقدان الوزن وطريقة مطيافية الممانعة الكهروكيمائية وتقنية قياس استقطابية فرق الجهد الديناميكي. أوضحت نتائج التجربة أن لدينة من نوع AFPP هي مانع فعال لتآكل الفولاذ الطري في وسط حمض الهيروكلوريك المولاري حيث أعطت كفاءة منع بنسبة 98%. و دللت قياسات استقطابية فرق الجهد الديناميكي على أن AFPP هو نوع من الموانع المختلطة التي يغلب عليها المنحى الكاثودي. وقد وجد أن إدمصاص (إمتزاز) مانع التآكل هذا على سطح الفولاذ الطري يتم وفقاً لقانون لانجمور للإدمصاص متساوي الحرارة. كذلك قد تم تعيين طاقة التنشيط (E_a) و طاقة الإدمصاص القياسية ($\Delta G°_{ads}$) وطاقة المحتوى الحراري (ΔH^*) وانتروبيا التنشيط (ΔS^*) لعملية التآكل.

Journal of the Association of Arab Universities for Basic and Applied Sciences (2015) **18**, 12–18

University of Bahrain

Journal of the Association of Arab Universities for Basic and Applied Sciences

www.elsevier.com/locate/jaaubas
www.sciencedirect.com

ORIGINAL ARTICLE

Effect of three component (aniline–formaldehyde and piperazine) polymer on mild steel corrosion in hydrochloric acid medium

K.R. Ansari, M.A. Quraishi *

Department of Chemistry, Indian Institute of Technology, Banaras Hindu University, Varanasi 221005, India

Received 29 August 2013; revised 4 April 2014; accepted 27 April 2014
Available online 20 June 2014

KEYWORDS

Mild steel;
EIS;
Corrosion;
Weight loss measurements

Abstract Polymeric Schiff base containing aniline, formaldehyde and piperazine (AFPP) was synthesized and investigated as corrosion inhibitor for mild steel in 1 M HCl by weight loss measurements, electrochemical impedance spectroscopy (EIS) and potentiodynamic polarization techniques. Experimental results showed that AFPP is an effective inhibitor for mild steel in 1 M HCl and exhibited 98% inhibition efficiency. Potentiodynamic polarization studies showed that AFPP is a mixed-type inhibitor predominantly cathodic type. The adsorption of inhibitor on the mild steel surface followed Langmuir adsorption isotherm. Activation energy (E_a), standard energy of adsorption ($\Delta G°_{ads}$), enthalpy of activation (ΔH^*), and entropy of activation (ΔS^*) of corrosion process were calculated and discussed.

1. Introduction

The corrosion inhibition of mild steel has tremendous technological importance due to its increased industrial applications (Ali et al., 2003). Corrosion is the serious problem that mankind is facing (Ahmad and MacDiarmd, 1996).

Acid has wide applications in industry such as in pickling, cleaning, decaling etc. To prevent the corrosion of the metal, inhibitors are extensively used. The selection of an inhibitor mainly depends upon its efficiency, economic feasibility and side effects on the environment.

The use of polymers as corrosion inhibitors has drawn considerable attention due to their inherent stability, cost effectiveness and better inhibition efficiency at a very low concentration (Umoren et al., 2008). Both natural and synthetic polymers have been used as corrosion inhibitors (Shukla and Quraishi, 2012). These polymers have high molecular weight and bulky structure due to this they can cover more area on the metal surface, which leads to high inhibition efficiency.

In continuation of our work on corrosion inhibition by polymers (El-Etre, 1998; Shukla et al., 2008; Quraishi and Shukla, 2009), we have reported the corrosion inhibition effect of polymer derived from aniline, formaldehyde and piperazine (AFPP) (Parveen et al., 2008) which increases the corrosion inhibition property at low concentration (100 mg L^{-1}) with inhibition efficiency of 98%.

In the present work we have studied the inhibitive effect of polymer derived from aniline, formaldehyde and piperazine (AFPP) on mild steel in 1 M hydrochloric acid (HCl) by using

* Corresponding author. Tel.: +91 9307025126; fax: +91 542 2368428.
E-mail addresses: maquraishi@rediffmail.com, maquraishi.apc@itbhu.ac.in (M.A. Quraishi).
Peer review under responsibility of University of Bahrain.

1815-3852 © 2014 Production and hosting by Elsevier B.V. on behalf of University of Bahrain.
http://dx.doi.org/10.1016/j.jaubas.2014.04.001

weight loss, electrochemical impedance spectroscopy (EIS), and potentiodynamic polarization techniques. According to literature survey, no work has been done on this compound as corrosion inhibitor.

2. Experimental

2.1. Materials and chemicals

The inhibitor under investigation has been synthesized elsewhere (Parveen et al., 2008). Its scheme of synthesis is shown in Fig. 1.

The corrosion test was performed on the mild steel strips containing (in wt.%) C: 0.076, P: 0.012, Si: 0.026, Mn: 0.192, Cr: 0.050, Cu: 0.135, Al: 0.023, Ni: 0.050 and remaining Fe. Mild steel strips used for weight loss measurement have dimension 2.5 cm × 2.0 cm × 0.025 cm. For electrochemical measurements, 7.5 cm long stem of mild steel strips with exposed surface area of 1.0 cm^2 (rest being coated with commercially available lacquer) was used. The test solution, 1 M HCl was prepared by dilution of analytical grade HCl with double distilled water. The inhibitor concentration ranges from 25 to 100 mg L^{-1}.

2.2. Methods

2.2.1. Weight loss measurements

The weight loss measurements of mild steel strips of size 2.5 cm × 2.0 cm × 0.025 cm were used in 1 M HCl without and with addition of different concentrations of inhibitor for 3 h at 308 K temperature without stirring. Following equations were used for the determination of inhibition efficiency $\eta\%$ and surface coverage (θ):

$$\eta\% = \frac{C_R - C_{R(i)}}{C_R} \times 100 \quad (1)$$

$$\theta = \frac{C_R - C_{R(i)}}{C_R} \quad (2)$$

where C_R and $C_{R(i)}$ are the values of the corrosion rates (mg cm^{-2} h^{-1}) of mild steel in the absence and presence of inhibitor, respectively.

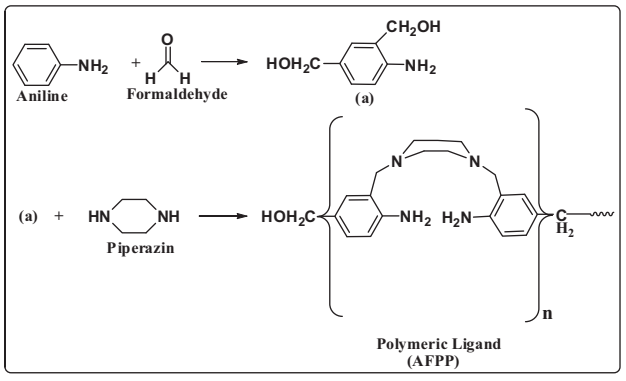

Figure 1 Scheme of ligand (AFPP) synthesis.

2.2.2. Electrochemical measurements

All electrochemical experiments were performed in Gamry electrochemical cell with three electrode cell, consisting of a mild steel rod of 1 cm^2 as working electrode, a platinum foil as counter electrode and standard calomel electrode (SCE) as a reference electrode, connected to Gamry Instrument Potentiostat/Galvanostat with a Gamry framework system based on ESA 400. Gamry applications include EIS 300 for EIS measurements, DC 105 software for corrosion and Echem Analyst (version 5.50) software package for data fitting. All potentials were measured versus SCE. The electrolyte used was 1 M HCl maintained at 308 K.

2.2.2.1. Electrochemical impedance spectroscopy (EIS). EIS measurements were carried out with Gamry Instrument Potentiostat/Galvanostat, which consists of a unit with a potentiostat and an acquisition system. The principle of this analytical technique consists of superposing a slight sinusoidal voltage ΔE sin ωt (10 mV peak to peak) from high to low frequency (10^5–10^{-2}Hz) to the potential applied to the sample.

2.2.2.2. Potentiodynamic polarization. Potentiodynamic polarization curves were obtained by changing the electrode potential automatically from −250 to +250 mV versus E_{OC} at a scan rate of 1 mV s^{-1}. All experiments were measured after immersion for 30 min in 1 M HCl in the absence and presence of inhibitor.

3. Experimental results and discussion

3.1. Weight loss measurements

3.1.1. Effect of inhibitor concentration

Effect of inhibitor (AFPP) concentration on the corrosion of mild steel in 1 M HCl was studied by weight loss measurement at 308 K and the results are given in Table 1.

The data in Table 1 reveal that as the concentration of AFPP increases inhibition efficiency increases (Karthikaiselvi and Subhashini, 2014) and corrosion rate decreases. This behavior can be attributed to the increase in surface area covered by the adsorbed molecules on the mild steel surface with an increase in the concentration of AFPP. The maximum efficiency of 98% was achieved at the concentration of 100 mg L^{-1}.

3.1.2. Effect of temperature

The inhibition efficiency in 1 M HCl at optimum concentration (100 mg L^{-1}) of AFPP at temperature ranging from 308 to 338 K was done and result obtained is given in Table 2.

Table 1 Parameters obtained from weight loss measurement for mild steel in 1 M HCl containing different concentrations of AFPP at 308 K.

Inhibitor	Concentration (mg L^{-1})	Corrosion rate (mg cm^{-2} h^{-1})	Surface coverage (θ)	η (%)
Blank	0.0	7.00	–	–
AFPP	25	1.60	0.771	77.1
	50	0.66	0.904	90.4
	75	0.30	0.957	95.7
	100	0.13	0.980	98.0

Table 2 Parameters obtained from weight loss measurement of mild steel in 1 M HCl containing optimum concentration of AFPP at different temperatures.

Inhibitor	Temperature (K)	Corrosion rate (mg cm^{-2} h^{-1})	η (%)
Blank	308	7.00	–
	318	9.66	–
	328	14.6	–
	338	18.7	–
AFPP	308	0.13	98.0
	318	0.43	95.5
	328	1.20	91.7
	338	3.06	83.62

From Table 2, it was found that the inhibition efficiencies decrease and corrosion rate increases with increasing temperature. This phenomenon can be explained with the desorption of adsorbed inhibitor molecules from the mild steel surface. Due to this greater surface area of mild steel comes in contact with corrosive environment which results in an increase in the corrosion rate (Fouda and Ellithy, 2009). The activation parameters were calculated by using Arrhenius equation (Tao et al., 2009).

$$C_R = A \exp\left(\frac{-E_a}{RT}\right) \tag{3}$$

where E_a is the activation energy, R is the gas constant, A is the pre-exponential factor.

Arrhenius plot for the corrosion rate of mild steel is given in Fig. 2a. Linear regression between log (C_R) and $1/T$ is used to calculate the value of activation energy E_a) for mild steel in 1 M HCl in the absence and presence of inhibitor, results are listed in Table 3.

From Table 3, it was found that the value of E_a is higher for inhibited solution than that for uninhibited. This higher value of E_a is obtained due to adsorbed inhibitor molecules which create physical barrier for charge and mass transfer (Martinez and Stern, 2002).

Enthalpy and entropy of activation can be calculated by using Arrhenius equation (Tao et al., 2009):

Table 3 Activation parameter for mild steel in 1 M HCl in the absence and presence of optimum concentration of AFPP.

Inhibitor	E_a (kJ mol^{-1})	ΔH^* (kJ mol^{-1})	ΔS^* (J K^{-1} mol^{-1})
Blank	27.9	25.4	−147.4
AFPP	90.3	87.7	43.0

$$C_R = \frac{RT}{Nh} \exp\left(\frac{\Delta S^*}{R}\right) \exp\left(-\frac{\Delta H^*}{RT}\right) \tag{4}$$

where h is Plank's constant, N is Avogadro's number, ΔS^* is the entropy of activation and $\Delta H^*$is the enthalpy of activation.

A plot of log C_R/T against $1/T$ gives straight lines with slope values of ($\Delta H^*/2.303R$)) and an intercept of [log(R/Nh)) + ($\Delta S^*/2.303R$)] as in Fig. 2a, from which the values of ΔH^* and ΔS^* were calculated and given in Table 3. The positive value of ΔH^*gives an evidence of endothermic nature of dissolution of mild steel, which suggests the slower dissolution of mild steel in the presence of inhibitor (Tao et al., 2009). As from Table 3, the sign of ΔS^* is negative in blank and positive in the presence of inhibitor. The adsorption of organic inhibitor molecules on the mild steel surface can be regarded as a quasi-substitution process between the organic compound in the aqueous phase [$Org_{(sol)}$] and water molecule on electrode (mild steel) surface [$H_2O_{(ads)}$] (Sahin et al., 2002) (Fig. 2b).

$$Org_{(sol)} + xH_2O_{(ads)} \leftrightarrow Org_{(ads)} + xH_2O_{(sol)}$$

where x is the size ratio, that is, the number of water molecules replaced by one organic inhibitor. In this situation, the adsorption of inhibitor is accompanied by desorption of water molecules from the surface. Therefore, the gain in entropy is attributed to the increase in solvent entropy and to more positive water desorption enthalpy (Branzoi et al., 2000; Ateya et al., 1984). The positive value of ΔS^* also means that disordering increases on going from reactants to the metal/solution interface (Banerjee and Malhotra, 1992), which is the driving force for the adsorption of inhibitor onto the mild steel surface (Li et al., 2008).

3.1.3. Adsorption considerations

In order to gain more information about the type of interaction between the inhibitor molecules and the mild steel surface,

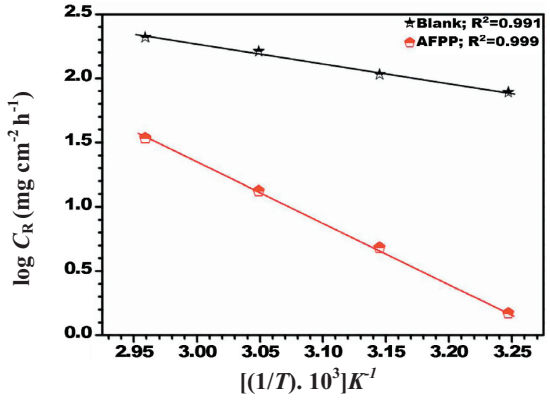

Figure 2a Arrhenius plot of mild steel in 1 M HCl in the absence and presence of optimum concentration of AFPP.

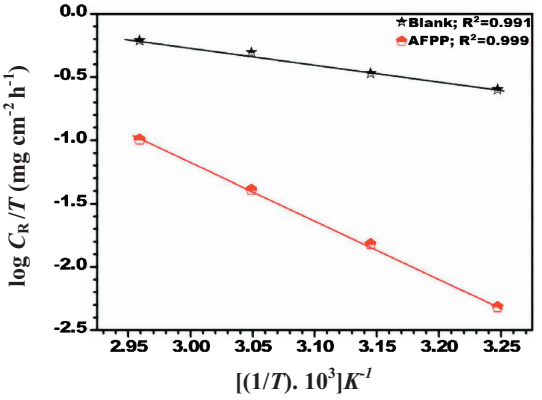

Figure 2b Transition-state plot of mild steel in 1 M HCl in the absence and presence of optimum concentration of AFPP.

different adsorption isotherms were tested. The Langmuir isotherm, Eq. (5), was found to fit well with the experimental data obtained from the investigated compound (Xometi et al., 2008).

$$K_{ads}C_{inh} = \frac{\theta}{1-\theta} \tag{5}$$

where θ is the surface coverage, C_{inh} is the inhibitor concentration (mg L^{-1}), K_{ads} is the equilibrium constant of adsorption process. The plot of C_{inh}/θ vs inhibitor concentration (C_{inh}) was evaluated and given in Fig. 2c.

3.2. Electrochemical measurements

3.2.1. AC technique: Electrochemical impedance spectroscopy

Nyquist plots of the inhibitor in 1 M HCl solution in the absence and presence of different concentrations of AFPP are given in Fig. 3a. The impedance spectra show a single semicircle and the diameter of semicircle increases with increasing inhibitor concentration. The impedance spectra consist of one capacitive loop from high frequency to low frequency, the high frequency capacitive loop was attributed to charge transfer of the corrosion process (Paskossy, 1994). From the figure it is noticed that the impedance spectra have a "depressed" semicircle at the center under the real axis, this phenomenon often refers to the frequency dispersion of interfacial impedance which has been attributed to the roughness; inhomogeneities of the solid surfaces and adsorption of inhibitor (Growcock and Jasinski, 1989; Bustamante et al., 2009).

The equivalent circuit model used to fit the experimental results is shown in Fig. 3b.

It consists of solution resistance (R_s), charge transfer resistance (R_{ct}) and constant phase element (CPE). The admittance, Y_{CPE}, and impedance, Z_{CPE}, are expressed as (Khaled, 2010).

$$Y_{\text{CPE}} = Y_0(j\omega)^n \tag{6}$$

$$Z_{\text{CPE}} = \left(\frac{1}{Y_0}\right)[(j\omega)^n]^{-1} \tag{7}$$

where Y_0 is the amplitude comparable to a capacitance, j is the square root of -1, ω is angular frequency ($\omega = 2\pi f_{\max}$), n is the phase shift, which can be used as a gauge of the heterogeneity or roughness of the mild steel surface. The CPE can be

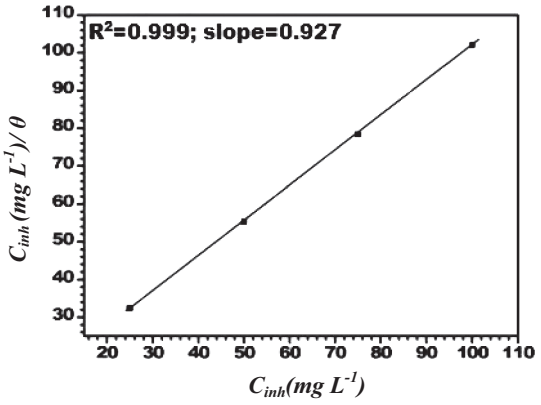

Figure 2c Langmuir's isotherm for adsorption of AFPP on the mild steel surface in 1 M HCl.

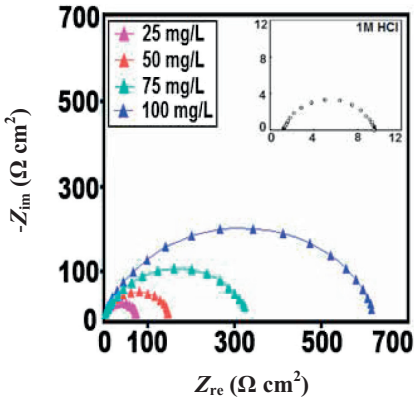

Figure 3a Nyquist plots for mild steel in 1 M HCl in the absence and presence of different concentrations of AFPP at 308 K.

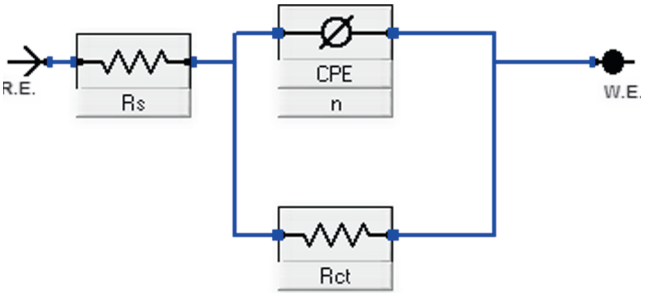

Figure 3b Equivalent circuit used to fit the EIS data.

expressed by the values of n if resistance ($n = 0$, $Y_0 = R$), capacitance ($n = 1$, $Y_0 = C$), inductance ($n = -1$, $Y_0 = L$) and Warburg impedance ($n = 0.5$, $Y_0 = W$) (Khaled and Amin, 2009).

The double layer capacitance (C_{dl}) values can be calculated from CPE parameter values Y and n using the following equation (Zhang et al., 2009).

$$C_{dl} = \frac{Y\omega^{n-1}}{\sin(n(\pi/2))} \tag{8}$$

The inhibition efficiency ($\eta\%$) using R_{ct} values was calculated from the equation (Quraishi et al., 2012).

$$\eta\% = \left(1 - \frac{R_{ct}}{R_{ct(i)}}\right) \times 100 \tag{9}$$

where $R_{\text{ct(i)}}$ and R_{ct} are the charge transfer resistance in the presence and absence of optimum concentration of AFPP.

According to the expression of the double layer capacitance presented in the Helmholtz model:

$$C_{\text{dl}} = \frac{\varepsilon\varepsilon_0}{d}S \tag{10}$$

where ε_0 is the permittivity of free space (8.854×10^{-12} F m^{-1}) and ε is the local dielectric constant of medium, S is the surface area of the electrode. Eq. (10) suggests that C_{dl} is inversely proportional to d.

It can be seen from Table 4 that the value of R_{ct} increases as the inhibitor concentration increases. The value of R_{ct} ranges from 59.7 to 618.5 Ω cm^2 and C_{dl} from 29.4 to 15.3 μF cm^{-2}. The large R_{ct} is associated with a slower corroding system, due to a decrease in the active surface necessary for the corro-

Table 4 Electrochemical impedance parameters for mild steel in 1 M HCl solution in the absence and presence of different concentrations of AFPP at 308 K.

Inhibitor (mg L^{-1})	R_s (Ω)	$R_{ct}n$ (Ω cm^2)	n	Y_0 (μF cm^{-2})	C_{dl} (μF cm^{-2})	θ	η (%)
Blank	1.02	7.44	0.798	481.2	137.9	–	–
25	1.45	59.7	0.874	56.1	29.4	0.795	79.5
50	0.857	139.1	0.828	72.5	25.8	0.912	91.2
75	0.688	319.4	0.780	66.8	24.5	0.961	96.1
100	0.992	618.5	0.808	35.4	15.3	0.980	98.0

sion reaction and the decrease in C_{dl} is due to the gradual replacement of water molecules by the adsorption of the AFPP at metal/solution interface, leading to the formation of protective film on the mild steel surface (Bentiss et al., 2000).

Fig. 3c shows the Bode impedance magnitude and the phase angle plots recorded for the mild steel in the absence and presence of different concentrations of AFPP at its open circuit potential in 1 M HCl. The impedance at high frequency limit (f = 10 kHz) corresponds to the ohmic resistances of the corrosion product film and the solution enclosed between the working electrode and the reference electrode (R_s). This resistive behavior is confirmed by 0° phase angle between current band potential at high frequency. However, at the low frequency limit the phase angle goes to negative value which corresponds to the inductive behavior (Hassan et al., 2007). This inductive behavior may occur due to the relaxation process obtained by adsorbed species like Cl^-_{ads} and H^+_{ads} on the electrode surface (Amin et al., 2007; Lenderrink et al., 1993; Kedam et al., 1981; Veloz and González, 2002; Sherif and Park, 2006). It may also occur due to the re-dissolution of the passivated surface at low frequencies (Yadav et al., 2012). As from Fig. 3c it is observed that at intermediate frequencies, a linear relationship between log|Z| vs log$f$ with a slope near −1 and the phase angle approaching −80° can be observed. This response is a characteristic of capacitive behavior. An ideal capacitive behavior would result in a slope of −1 and a phase angle of −90° at intermediate frequencies (Hassan et al., 2007). This accounts for the deviation from ideal capacitive behavior at intermediate frequencies (Macdonald et al., 2005) and occurs due to the increase of the standard rate constant of the barrier layer dissolution.

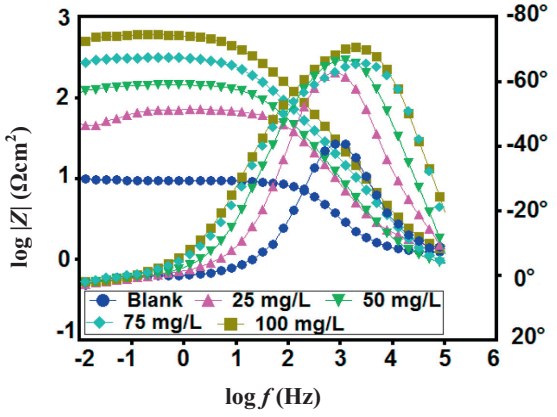

Figure 3c Bode impendence plots for mild steel in 1 M HCl in the absence and presence of different concentrations of AFPP at 308 K.

In the beginning of the immersion the gradual approach of $-S$ and $-\alpha°$ to the ideal capacitive values may be related to slowing down the rate of dissolution with time. For the same reason, in the presence of inhibitor (Table 5) there is the faster attaining of steady state of $-S$ and $-\alpha°$ and their higher values correspond to the catalytic action of the inhibitor in the mild steel dissolution process (Maranhao et al., 2006). The Bode phase angle plots show single maximum (one time constant) at intermediate frequencies, which is slightly broadened in the presence of inhibitor which may be due to the formation of a protective layer (Solmaz et al., 2008).

3.2.2. DC techniques: Tafel and linear polarizations

Polarization curves for mild steel/inhibitor interface in 1 M HCl at 308 K in the absence and presence of different concentrations of AFPP are shown in Fig. 4.

The corrosion inhibition efficiency was calculated by using the following equation (McCafferty and Hackerman, 1972):

Table 5 The slopes of the Bode impedance magnitude plots at intermediate frequencies (S) and the maximum phase angles (α) for mild steel in 1 M HCl solution at different concentrations of AFPP at 308 K.

Inhibitor (mg L^{-1})	$-S$	$-\alpha°$
Blank	0.502	40.90
25	0.788	63.02
50	0.750	66.78
75	0.707	65.66
100	0.790	70.67

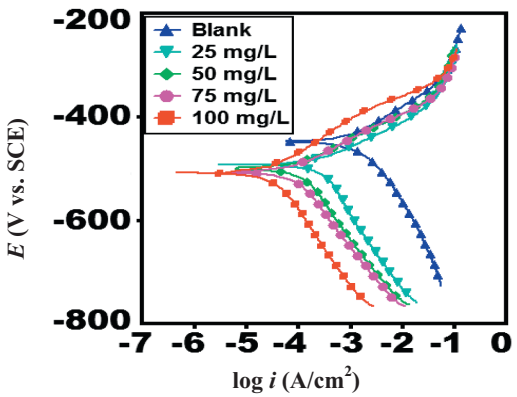

Figure 4 Potentiodynamic polarization curves for mild steel in 1 M HCl in the absence and presence of different concentrations of AFPP at 308 K.

Table 6 Electrochemical polarization parameters for mild steel in 1 M HCl solution in the absence and presence of different concentrations of AFPP at 308 K.

Inhibitor (mg L^{-1})	I_{corr} (μA cm^{-2})	E_{corr} (mV/SCE)	β_a (mV/dec)	$-\beta_c$ (mV dec)	θ	η (%)
Blank	892	−444	61.0	81.0	–	–
25	301	−490	54.6	185.0	0.662	66.2
50	117	−498	57.8	151.0	0.868	86.8
75	92.3	−506	60.5	147.0	0.896	89.6
100	25.5	−505	69.1	138.2	0.971	97.1

$$\eta\% = \left(1 - \frac{I_{corr(i)}}{I_{corr}}\right) \times 100 \quad (11)$$

where I_{corr} and $I_{corr(i)}$ are the uninhibited and inhibited corrosion current densities, respectively.

The complete electrochemical parameters E_{corr}, I_{corr}, anodic and cathodic Tafel slopes (β_a, β_c), inhibition efficiency were calculated by polarization measurements and listed in Table 6.

The values of β_c are more negative with respect to blank and changed with increasing inhibitor concentration (Fig. 4 and Table 6), which indicates the influence of the inhibitor on the kinetics of hydrogen evolution. If the deviation in E_{corr} is greater than 85 mV in inhibited system with respect to uninhibited, the inhibitor could be recognized as cathodic or anodic type (Bammou et al., 2014) whereas if the deviation in E_{corr} is less than 85 mV, it could be recognized as mixed type of inhibitor. Since the deviation in E_{corr} in our case is less than 85 mV, the inhibitor is mixed type but predominantly cathodic. (Xometi et al., 2008).

From Table 6 it is observed that the anodic Tafel slope slightly changes upon addition of inhibitor which may have occurred due to the chloride ions/or inhibitor molecules adsorbed onto the mild steel surface (Cao, 2004). Table 6 reveals that the corrosion current (I_{corr}) decreases and η% increases with the increase of inhibitor concentrations (Xometi et al., 2008).

3.2.2.1. Explanation of inhibition. The nature of adsorption and inhibition of a given inhibitor is a complex phenomenon and it cannot be explained by a single adsorption mode as given in Fig. 5. The adsorption and inhibition effect of inhibitor in HCl solution can be explained as follows:

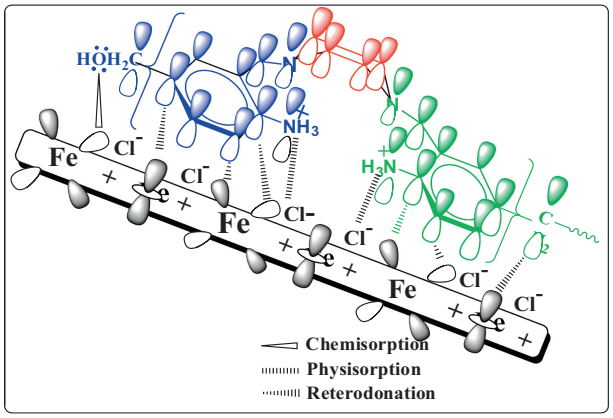

Figure 5 Mechanism of inhibition.

1. Inhibitor might be protonated in the acid solution as follows:

$$AFPP + xH+ \leftrightarrow [AFPPH_x]^{x+}$$

2. The protonated inhibitor may adsorb through electrostatic interactions between the positively charged molecules and the negatively charged metal surface, i.e. there may be a synergism between Cl^- and protonated inhibitor.
3. This physically adsorbed protonated inhibitor molecules undergo competition with H^+ ions for electrons on the mild steel surface. Cationic form of inhibitor returns to its neutral state after release of H_2 gas and heteroatoms with free lone pair electrons promote chemical adsorption.
4. Also the electron from d-orbital of Fe might be transferred to vacant π^* (antibonding) orbital of inhibitor molecules (reterodonation) and which strengthen adsorption.
5. Protonated inhibitor molecules may combine with freshly generated Fe^{2+} ions on the mild steel surface forming metal inhibitor complexes which is as follows:

$$Fe \rightarrow Fe^{2+} + 2e^-$$

$$AFPP + Fe^{2+} \rightarrow [AFPP - Fe]^{2+}$$

$$[AFPP_x]^{x+} + Fe^{2+} \rightarrow [AFPP_x - Fe]^{(2+x)+}$$

4. Conclusion

The studied inhibitor shows excellent inhibition properties for corrosion of mild steel in 1 M HCl and its inhibition efficiency increases with increasing the concentration. The results obtained from weight loss measurements, polarization curves and electrochemical impedance study (EIS) are in reasonable agreement. The adsorption of the inhibitor obeys Langmuir adsorption isotherm. The result of polarization measurement demonstrated that the inhibitor under investigation is mixed-type but predominantly cathodic. The positive sign of ΔH^* indicates that the adsorption process is endothermic.

Acknowledgements

K. R. Ansari gratefully acknowledges Council of Scientific and Industrial Research (CSIR), New Delhi, India for the financial assistance and facilitation of the study.

References

Ahmad, N., MacDiarmd, A.G., 1996. Inhibition of corrosion of steels with the exploitation of conducting polymers. Synth. Met. 78 (2), 103–110.

Ali, S.A., Saeed, M.T., Rahman, S.V., 2003. The isoxazolidines: a new class of corrosion inhibitors of mild steel in acidic medium. Corros. Sci. 45 (2), 253–266.

Amin, M.A., Abd El-Rehim, S.S., El-Sherbini, E.E.F., Bayyomi, R.S., 2007. The inhibition of low carbon steel corrosion in hydrochloric acid solutions by succinic acid: Part I. Weight loss, polarization, EIS, PZC, EDX and SEM studies. Electrochim. Acta 52 (11), 3588–3600.

Ateya, B., El-Anadauli, B., El. Nizamy, F., 1984. The adsorption of thiourea on mild steel. Corros. Sci. 24 (6), 509–515.

Bammou, L., Belkhaouda, M., Salghi, R., Benali, O., Zarrouk, A., Zarrok, H., Hammouti, B., 2014. Corrosion inhibition of steel in sulfuric acidic solution by the chenopodium ambrosioides extracts. J. Assoc. Arab Univ. Basic Appl. Sci. 16, 83–90.

Banerjee, G., Malhotra, S.N., 1992. Contribution to adsorption of aromatic amines on mild steel surface from hcl solutions by impedance, UV, and raman spectroscopy. Corrosion 48 (1), 10–15.

Bentiss, F., Traisnel, M., Lagrenée, M., 2000. The substituted 1,3,4-oxadiazoles: a new class of corrosion inhibitors of mild steel in acidic media. Corros. Sci. 42 (1), 127–146.

Branzoi, V., Branzoi, F., Baibarac, M., 2000. The inhibition of the corrosion of Armco iron in HCl solutions in the presence of surfactants of the type of N-alkyl quaternary ammonium salts. Mater. Chem. Phys. 65 (3), 288–297.

Bustamante, R.A., Silve, G.N., Quijano, M.A., Hernandez, H.H., Romo, M.R., Cuan, A., Pardave, M.P., 2009. Electrochemical study of 2-mercaptoimidazole as a novel corrosion inhibitor for steels. Electrochim. Acta 54 (23), 5393–5399.

Cao, C.N., 2004. Corrosion Electrochemistry Mechanism. Chemical Industrial Engineering Press, Beijing, p. 235 (in Chinese).

El-Etre, A.Y., 1998. Natural honey as corrosion inhibitor for metals and alloys. I. Copper in neutral aqueous solution. Corros. Sci. 40 (11), 1845–1850.

Fouda, A., Ellithy, A.S., 2009. Inhibition effect of 4-phenylthiazole derivatives on corrosion of 304L stainless steel in HCl solution. Corros. Sci. 51 (4), 868–875.

Growcock, F.B., Jasinski, J.H., 1989. Time-resolved impedance spectroscopy of mild steel in concentrated hydrochloric acid. Electrochem. Soc. 136 (8), 2310–2314.

Hassan, H.H., Abdelghani, E., Amin, M.A., 2007. Inhibition of mild steel corrosion in hydrochloric acid solution by triazole derivatives: Part I. Polarization and EIS studies. Electrochim. Acta 52 (22), 6359–6366.

Karthikaiselvi, R., Subhashini, S., 2014. Study of adsorption properties and inhibition of mild steel corrosion in hydrochloric acid media by water soluble composite poly (vinyl alcohol-o-methoxy aniline). J. Assoc. Arab Univ. Basic Appl. Sci. 16, 74–82.

Kedam, M., Mattos, O.R., Takenouti, H., 1981. Reaction model for iron dissolution studied by electrode impedance: I. Experimental results and reaction model. J. Electrochem. Soc. 128 (2), 257–266.

Khaled, K.F., 2010. Studies of iron corrosion inhibition using chemical, electrochemical and computer simulation techniques. Electrochim. Acta 55 (22), 6523–6532.

Khaled, K.F., Amin, M.A., 2009. Corrosion monitoring of mild steel in sulphuric acid solutions in presence of some thiazole derivatives – Molecular dynamics, chemical and electrochemical studies. Corros. Sci. 51 (9), 1964–1975.

Lenderrink, H.J.W., Linden, M.V.D., De Wit, J.H.W., 1993. Corrosion of aluminium in acidic and neutral solutions. Electrochim. Acta 38 (14), 1989–1992.

Li, X.H., Deng, S.D., Fu, H., Mu, G.N., 2008. Synergistic inhibition effect of rare earth cerium(IV) ion and anionic surfactant on the corrosion of cold rolled steel in H_2SO_4 solution. Corros. Sci. 50 (9), 2635–2645.

Macdonald, D.D., Barsoukov, E., Macdonald, J.R. (Eds.), 2005. Wiley Interscience, New York, p. 408.

Maranhao, S.L.A., Guedes, I.C., Anaissi, F.J., Toma, H.E., Aoki, I.V., 2006. Electrochemical and corrosion studies of poly (nickel-tetraaminophthalocyanine) on carbon steel. Electrochim. Acta 52 (2), 519–526.

Martinez, S., Stern, I., 2002. Thermodynamic characterization of metal dissolution and inhibitor adsorption processes in the low carbon steel/mimosa tannin/sulfuric acid system. Appl. Surf. Sci. 199 (1–4), 83–89.

McCafferty, E., Hackerman, N., 1972. Double layer capacitance of iron and corrosion inhibition with polymethylene diamines. J. Electrochem. Soc. 119 (2), 146–154.

Parveen, S., Ahamad, T., Malik, A., Nishat, N., 2008. Antimicrobial activity of aniline-formaldehyde resin modified by adding piperazine moiety and its metal polychelates. Polym. Adv. Technol. 19, 1779–1786.

Paskossy, T., 1994. Impedance of rough capacitive electrodes. J. Electroanal. Chem. 364 (1–2), 111–125.

Quraishi, M.A., Shukla, S.K., 2009. Poly(aniline-formaldehyde): a new and effective corrosion inhibitor for mild steel in hydrochloric acid. Mater. Chem. Phys. 113 (2–3), 685–689.

Quraishi, M.A., Ansari, K.R., Ebenso, Eno, E., 2012. A new and effective macrocyclic compound as corrosion inhibitor for mild steel in hydrochloric acid solution. Int. J. Electrochem. Sci. 7, 13106–13120.

Sahin, M., Bilgic, S., Yılmaz, H., 2002. The inhibition effects of some cyclic nitrogen compounds on the corrosion of the steel in NaCl mediums. Appl. Surf. Sci. 195 (1–4), 1–7.

Sherif, E.M., Park, S.M., 2006. Effects of 1,4-naphthoquinone on aluminum corrosion in 0.50 M sodium chloride solutions. Electrochim. Acta 51 (7), 1313–1321.

Shukla, S.K., Quraishi, M.A., 2012. Effect of some substituted anilines-formaldehyde polymers on mild steel corrosion in hydrochloric acid medium. J. Appl. Polym. Sci. 124, 5130–5137.

Shukla, S.K., Quraishi, M.A., Prakash, R., 2008. A self-doped conducting polymer ''polyanthranilic acid'': an efficient corrosion inhibitor for mild steel in acidic solution. Corros. Sci. 50 (10), 2867–2872.

Solmaz, R., Kardas, G., Culha, M., Yazici, B., Erbil, M., 2008. Investigation of adsorption and inhibitive effect of 2-mercaptothiazoline on corrosion of mild steel in hydrochloric acid media. Electrochim. Acta 53 (20), 5941–5952.

Tao, Z., Zhang, S., Li, W., Hou, B., 2009. Corrosion inhibition of mild steel in acidic solution by some oxo-triazole derivatives. Corros. Sci. 51 (11), 2588–2595.

Umoren, S.A., Ogbobe, O., Igwe, I.O., Ebenso, E.E., 2008. Inhibition of mild steel corrosion in acidic medium using synthetic and naturally occurring polymers and synergistic halide additives. Corros. Sci. 50 (7), 1998–2006.

Veloz, M.A., González, I., 2002. Electrochemical study of carbon steel corrosion in buffered acetic acid solutions with chlorides and H_2S. Electrochim. Acta 48 (2), 135–144.

Xometi, O.O., Likhanova, N.V., Anguilar, M.A.D., Arce, E., Dorantes, H., Lozada, P.A., 2008. Synthesis and corrosion inhibition of α-amino acids alkylamides for mild steel in acidic environment. Mater. Chem. Phys. 110 (2–3), 344–351.

Yadav, D.K., Quraishi, M.A., Maiti, B., 2012. Inhibition effect of some benzylidenes on mild steel in 1 M HCl: an experimental and theoretical correlation. Corros. Sci. 55, 254–266.

Zhang, S., Tao, Z., Li, W., Hou, B., 2009. The effect of some triazole derivatives as inhibitors for the corrosion of mild steel in 1 M hydrochloric acid. Appl. Surf. Sci. 255 (15), 6757–6763.